BMC Cardiovascular Disorders

RESEARCH

Open Access

Ventricular arrhythmias originating from different portions of the communicating vein of the left ventricular summit: electrocardiographic characteristics and catheter ablation

Bing Shen[1,2†], Wu-Ming Hu[1†], Jia-Meng Shao[1], Yu Shen[1], Yu Yan[1], Shea Michaela James[1], Lucia D'Angelo[1], Guo-Juan Xu[1], Cheng Zheng[1*] and Jia-Feng Lin[1*]

Abstract

Background Idiopathic ventricular arrhythmias (IVAs) arising from different portions of the communicating vein of the left ventricular summit (summit-CV) are not a rare phenomenon. Whereas its electrocardiographic (ECG) and electrophysiological characteristics are not fully investigated.

Objective This study aimed to identify distinct ECG and electrophysiological features of IVAs originating from different portions of summit-CV.

Methods Nineteen patients confirmed arising from summit-CV were included in this study.

Results The 19 patients were divided into proximal and distal portion groups based on their target sites in summit-CV. In the proximal portion group, 100% (11/11) VAs showed dominant negative (rs or QS) waves in lead I, while in the distal portion group, 87.5% (7/8) showed dominant positive waves (R, Rs or r) ($p < 0.000$). In lead V_1, 100% (11/11) of the proximal portion group showed dominant positive waves (R or Rs), while 62.50% (5/8) of the distal portion group showed positive and negative bidirectional or negative waves (RS or rS) ($p < 0.005$). R_I>4mV, S_I<3.5mV, R_{V1}<13mV, S_{V1}>3.5mV, R_I/S_I>0.83, and R_{V1}/S_{V1}< 2.6 indicated a distal portion of summit-CV with the predictive value of 0.909, 1.000, 0.653, 0.972, 0.903, 0.966, respectively. A more positive wave in lead I and a more negative wave in lead V_1 indicated more distal origin in summit-CV. Target sites in proximal and distal summit-CV groups showed similar electrophysiological characteristics during mapping.

†Bing Shen and Wu-Ming Hu contributed equally to this work.

*Correspondence:
Cheng Zheng
zhengcheng_wzmufey@163.com
Jia-Feng Lin
linjiafeng_wzmcfey@163.com

Full list of author information is available at the end of the article

Conclusions There were significant differences in ECG characteristics of VAs at different portions of summit-CV, which could aid pre-procedure planning and facilitate radiofrequency catheter ablation (RFCA) procedures.

Keywords Catheter ablation, Ventricular arrhythmias, Summit-CV, Electrocardiogram, Bipolar intracardiac electrogram, Left ventricular summit

Introduction

Idiopathic ventricular arrhythmias (IVAs), including premature ventricular complexes (PVCs) and ventricular tachycardias (VTs), occur in patients without structural heart disease. In recent years, the radiofrequency catheter ablation (RFCA) of the left ventricular outflow tract (LVOT) VAs through aortic artery sinus cusp (ASC) and the distal great cardiac vein (DGCV) have been reported on, along with their ECG characteristics, ablation methods, and precautions [1, 2]. However, the ECG characteristics and ablation treatment of VAs from an extended branch of the DGCV, namely the summit-CV, have not been thoroughly investigated. This study aims to investigate the ECG characteristics of VAs originating from different portions of summit-CV, the bipolar intracardiac electrogram (bi-EGM) characteristics of effective target sites, and the results of ablation treatment.

Methods

Study population

From May 2010 to October 2022, a total of 3858 patients (mean age 49.43±17.39 years) with VAs who underwent RFCA in the Second Affiliated Hospital of Wenzhou Medical University were retrospectively reviewed. Among them, 27 patients were confirmed to have the effective target located in the summit-CV, and 19 patients were successfully ablated in the summit-CV. All patients met the guideline criteria for radiofrequency ablation of tachyarrhythmias. Before RFCA, a 12-lead ECG and 24-hour ambulatory ECG monitoring (Holter) were performed. At the same time, the following conditions were excluded: (1) Severe heart, lung, liver, or kidney insufficiency and coagulation dysfunction could not tolerate surgery; (2) The course of viral myocarditis or myocardial infarction or stroke less than half a year; (3) With malignant tumor, life expectancy less than one year; (4) Severe thoracic deformity; (5) Advanced age (>90 years old). Before the ablation, all AADs were withdrawn at least five half-lives. All subjects gave written informed consent. Studies and data collection were performed according to protocols approved by the Ethics Committee of the Second Affiliated Hospital of Wenzhou Medical University.

ECG analysis

The simultaneous 12-lead ECGs during the VAs and pace mapping were recorded digitally at a sweep speed of 100 mm/s in all patients for offline analysis. The following ECG features were assessed in patients with VAs originating from different portions of summit-CV: (1) the QRS morphology of the VAs in all 12 leads; (2) the site of R wave transition in the precordial leads; (3) the QRS complex duration; (4) the amplitude of QRS of the VAs.

Electrophysiological study and radiofrequency ablation

Under the guidance of a three-dimensional mapping system and X-ray image, a quadripolar saline-irrigated tip ablation catheter was sent through the right femoral vein and/or femoral artery to the right and left ventricle to perform activation mapping and pace mapping. A decapolar coronary sinus (CS) catheter was delivered as distal as possible in the coronary venous system when a DGCV-AIV or summit-CV origin of VAs was considered. If clinical VAs were absent during the procedure, intravenous isoproterenol or electrical stimulation was administered to induce VAs. The ideal target site of RFCA was determined by the earliest local activation time in bipolar EGM with QS pattern in unipolar EGM. If the ideal target was not identified at the endocardium of both ventricles or ablation was ineffective, mapping and ablation were performed through the CS to the great cardiac vein (GCV) and its branches. When manipulating the catheter in the coronary sinus and its branches, coronary venography (CVG) assisted visualization of the morphology and course of the coronary venous system and Swartz sheath support further stabilized the catheter movement. Coronary angiography (CAG) was performed before ablation to evaluate the distance between target sites and coronary arteries when target sites were considered adjacent to the coronary artery. Energy delivery was forbidden at the site within 5 mm of the coronary artery. CAG was performed again to assess the patency of coronary arteries. Ablation parameters of preset temperature of 43 ∘C, preset power of 25–35 W, flow rate of 30–60 mL/min, and impedance limit of 300 Ω was commonly applied. If a much higher impedance restrained the energy delivery, we increased the saline flow rate to reduce the impedance and adjust the upper impedance limit as high as possible [3]. Effective ablation was defined as the termination of VA within 10 s of energy delivery, or frequent PVC or paroxysmal VT with the same morphology as spontaneous VA occurred and quickly disappeared. The effective sites were discharged for another 60 ~ 90 s. The endpoint of the procedure was the disappearance of VAs and no longer induced through isoproterenol and electrical stimulation 30 min after the final energy application. If VAs

did not terminate within 10 s of energy delivery, remapping was performed to search for other target sites.

We defined acute success as the absence of spontaneous or provoked clinical VAs at the end of the procedure and during the latter 48-h period post-ablation on Holter without antiarrhythmic drugs (AADs).

Bipolar intracardiac electrogram recording and analytical method

GE's electrophysiological recorder (Prucka, USA) was used to record the intracardiac electrogram with a paper speed of 100 mm/s and a magnification of 64 times. For target sites, the A/V ratio during sinus rhythm in bi-EGM, and the specific bi-EGM characteristics of V wave in PVC were analyzed. The A/V ratio during sinus rhythm was defined as the following:①Large A wave and small V wave, A/V ratio > 1;②A wave = V wave, A/V ratio = 1; ③Small A wave and large V wave, A/V ratio < 1. According to characteristics, morphology, amplitude, and duration of the specific potentials in V wave, we further defined them as the following, which was described in detail in our previous study [4]: (I) presystolic short-duration fractionated potential, (II) presystolic long-duration multicomponent fractionated potential, (III) presystolic high-amplitude discrete potential, (IV) presystolic isolated discrete potential (V) NA: no specific potentials before V wave were recorded in bi-EGMs.

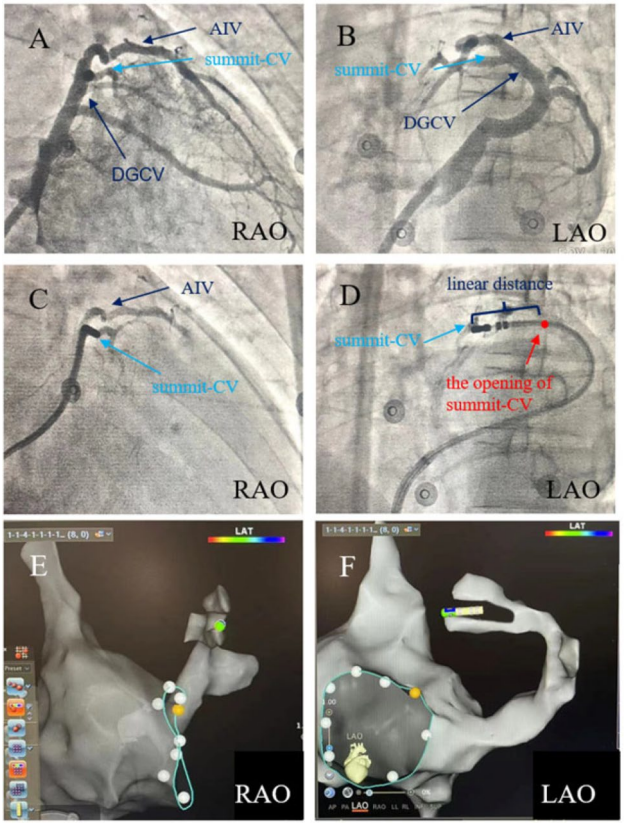

Fig. 1 Anatomical and imaging features of summit-CV. **A**, **B**: Coronary venography allowed clear visualization of the coronary venous architecture. **C**, **D**: In the LAO view, the catheter tip was engaged into the target site, and the linear distance from the target sites to the opening of summit-CV was precisely measured using standard catheter reference sizing. **E**, **F**: The three-dimensional mapping map of the summit of the left ventricle and summit-CV. DGCV, distal great cardiac vein; AIV, anterior interventricular vein; summit-CV, communicating vein of the left ventricular summit; LAO, left anterior oblique; RAO, right anterior oblique

Anatomic definitions

The Coronary vein has a complex anatomy with a tortuous shape, numerous branches, and significant variations. CVG could be used to clarify the anatomical structure of the coronary vein. The GCV was an extension of the CS, running in the coronary sulcus. Its distal end (DGCV) was located in the epicardium adjacent to the anterior septum of the mitral annulus, which was divided into two branches. One of which ran along the anterior interventricular sulcus and was accompanied by the left anterior descending artery (LAD) was the Anterior interventricular vein (AIV). The other one which originated from the intersection of DGCV and AIV, was located between the aortic and pulmonary annulus, and drained into the small cardiac vein, was known as summit-CV.

From the X-ray images, the course of summit-CV and AIV was different in the right anterior oblique position (RAO); the former was behind the RVOT, and the latter was in front of the RVOT and went forward and downward along the anterior ventricular groove (Fig. 1A and C). In the left anterior oblique position (LAO), the AIV extended from the DGCV and went further down in the middle of the cardiac silhouette; the summit-CV was situated on the rightward of the intersection of DGCV and AIV (Fig. 1B and D). In Fig. 1E and F, the three-dimensional mapping map of the summit of the left ventricle and summit-CV. Summit-CV visualized by the three-dimensional mapping system (Fig. 1E LAO and 1 F RAO).

Groups

The linear distance between the target sites in summit-CV and the intersection of DGCV and AIV was measured using standard catheter reference sizing with an 8 F catheter diameter, in the LAO view (Fig. 1D). All measurements were performed by three electrophysiologists independently, and the average value was finally adopted. The VAs were divided into two groups, the proximal group (≤10 mm) and the distal group (>10 mm), based on the linear distance between the target sites in summit-CV and the intersection of DGCV and AIV.

Follow-up

After RFCA, AADs were stopped and routine ECG monitoring was performed for 24 h. All patients were followed up by echocardiography (UCG) and DCG 3 months

post-ablation. Later, patients were followed up every 3 to 6 months.

Statistical analysis

Categorical variables were expressed as case numbers and percentages. Measurement data were expressed as mean±standard deviation. For normal distribution data, the student's *t-test* was used to compare two groups, and the analysis of variance (ANOVA) and Cochran's q-test were used to compare multiple groups. Categorical variables were compared using the Pearson χ^2 test or Fisher's exact test when appropriate. Receiver-operating characteristic curves were used to obtain the best sensitivity and specificity values. A value of $P<0.050$ was considered significant.

Result

Patient characteristics

Between May 2010 and October 2022, 27 patients were found to have IVAs originating from the summit-CV at our center. In two cases, it was confirmed that the effective target was located in the summit-CV using the decapolar CS catheter. Still, the ablation catheter failed to reach the effective target due to the thin lumen of the summit CV. Three cases were unsuccessful because the distance between the target and the LAD was less than 5 mm, prohibiting ablation. Additionally, three cases failed because of high impedance that could not be overcome with any available methods. For these patients, ablation was attempted at adjacent sites in the closest proximity to the earliest activation site, such as the cusps, LVOT, and RVOT. The remaining 19 patients (12 males; mean age 56.81±14.62 years) achieved successful ablation at the effective target in the summit-CV. The clinical characteristics of the patients are given in Table 1. All patients had been treated with 2 to 3 kinds of AADs, which were ineffective and significantly affected the quality of life. The chest X-ray, UCG, CAG, and cardiac magnetic resonance excluded structural abnormalities. There were no significant differences concerning age, gender, course of the disease, the total number of PVCs, comorbidities such as hypertension and diabetes, left ventricular enlargement, and type of VA between patients with VAs in two groups ($p>0.050$). The 19 VAs were divided into the proximal group (11 cases) and the distal group (8 cases), based on the distance of effective target sites in the summit-CV to the intersection of the AIV and DGCV.

Common ECG characteristics

The common ECG features of VA in both groups were characterized by R-type QRS waves in leads II, III, aVF, and V4-V6, whereas leads aVR and aVL showed a QS-type pattern.

Comparison of ECG characteristics between the two groups

Significant differences were observed in QRS morphology, R(S) wave amplitude, and R/S ratio in leads I and V_1 between the two groups (Table 2; Fig. 2). ① In the proximal portion group, all 11 patients (100%) had rs or QS type with mainly negative waves, while in the distal portion group, 87.5% (7/8) QRS morphology in lead I was R, Rs or r type with mainly positive wave ($p<0.000$); ② In lead V_1, 100% (11/11) of the proximal portion group showed mainly positive waves and R or Rs type, while 62.50% (5/8) of the distal portion group showed mainly positive and negative bidirectional or negative waves and RS or rS type ($p<0.005$).

The comparison of R(S) wave amplitude and R/S ratio in leads I and V_1 between the two groups is shown in Table 2. Except for R_{V1} amplitude, R_I and S_{V1} amplitude, and ratios of R_I/S_I in the distal group were significantly higher than those in the proximal group (Z=-3.470~-2.980, $p<0.001\sim0.003$), while S_I amplitude and ratios of R_{V1}/S_{V1} in the proximal group were considerably higher than that in the distal group (Z=-3.741~-3.388, $p<0.000\sim0.001$). Table 2 shows the total QRS duration and the peak deflection index (PDI) [5] in two groups had no statistical significance.

Mapping and ablation

The results of the mapping and ablation of the two groups are shown in Table 3. There were no significant differences in activation mapping V-QRS time, pacing similarity, number of ablation attempts, discharge time, and X-ray exposure time between the two groups ($p>0.050$). However, the operation time was longer in the distal

Table 1 Comparison of clinical characteristics between the two groups [n (%), $\bar{X}\pm S$]

	Gender (men %)	Age (years old)	The course of disease (year)	Total number of PVCs (times/24 h)	Hypertension, *n* (%)	Diabetes, *n* (%)	Left ventricular enlargement, *n* (%)	PVCs, *n*(%)
The proximal group ($n=11$)	7(63.64)	56.1±14.4	2.9±2.0	23,515±8043	2(18.18)	1(9.09)	1(9.09)	10(90.91)
The distal group ($n=8$)	5(62.50)	57.8±14.2	3.1±2.3	23,958±8296	1(12.50)	1(12.50)	1(12.50)	7(87.50)
p	0.16	0.2508	0.1941	0.0881	/	/	/	/
t	>0.5	>0.5	>0.5	>0.5	>0.05	>0.05	>0.05	>0.05

PVCs=premature ventricular complexes

Table 2 Comparison of ECG characteristics, R (S) wave amplitude and R/S ratio in leads I and V_1 between the two groups (n %)

		The proximal group ($n=11$)	The distal group ($n=8$)	Z	p
QRS morphology in lead I	r	0	2 (25.00)	/	< 0.000
	R	0	2 (25.00)		
	Rs	0	3 (37.50)		
	rs	6 (54.55)	1 (12.50)		
	QS	5 (45.45)	0		
QRS morphology in lead V_1	R	5 (45.45)	0	/	< 0.005
	Rs	6 (54.55)	3 (37.50)		
	RS	0	4 (50.00)		
	rS	0	1 (12.50)		
QRS morphology in lead V_2	R	2 (18.18)	0	/	> 0.05
	Rs	4 (36.36)	4 (50.00)		
	RS	5 (45.45)	3 (37.50)		
	rS	0	1 (12.50)		
Amplitude of R_I (mv)		1.77 ± 1.94	6.00 ± 2.39	-3.008	0.003
Amplitude of S_I (mv)		5.91 ± 0.92	1.75 ± 1.56	-3.741	0.000
R_I/S_I ratio		0.30 ± 0.33	2.94 ± 2.69	-2.980	0.003
Amplitude of R_{V1}(mv)		13.09 ± 4.89	9.75 ± 2.76	-1.136	0.256
Amplitude of S_{V1}(mv)		1.77 ± 1.94	9.56 ± 5.08	-3.470	0.001
R_{V1}/S_{V1} ratio		8.75 ± 6.32	1.41 ± 0.91	-3.388	0.001
Total QRS duration		153.1 ± 11.7	143.4 ± 10.6	/	0.08
PDI		0.59 ± 0.06	0.59 ± 0.05	/	> 0.5

group ($p=0.03$), and the linear distance from the summit-CV opening was longer in the distal group ($p<0.000$). In addition, it was observed in bipolar intracardiac electrograms that there were differences in the characteristics between the proximal and distal groups: ① In the proximal group, the bipolar intracardiac electrograms A/V ratio equal to 1 and less than 1 were 36.36% (4/11) and 63.64% (7/11), respectively, while all were less than 1 in the distal group; ② The incidence of specific potentials in bipolar intracardiac electrograms at effective target in the proximal and distal groups were 81.81% (9/11) and 87.50% (7/8), respectively; ③ Pacing mapping captured ventricles in the proximal and distal groups were 90.91% (10/11) and 87.50% (7/8). However, the difference was not statistically significant.

During the procedure, coronary vein dissection occurred in 1 case (5.26%). In the case of other complications, such as coronary vein rupture, pericardial effusion, pericardial tamponade, or acute coronary artery injury, none were observed. All patients were followed up for 3 months to 6 years, with an average of 2.7 ± 2.1 years, and no recurrence was found.

ROC curves and scatter plots of R(S) wave amplitude and R/S ratio in leads I and V1

Receiver operating characteristic analyses determined that R_I >4mV, S_I <3.5mV, R_{V1} <13mV, S_{V1} >3.5mV, R_I/S_I >0.83, and R_{V1}/S_{V1} < 2.6 indicated VAs originating from the distal portion of summit-CV with predictive value of 90.9%, 100%, 65.3%, 97.2%, 90.3%, 96.6%, respectively (Fig. 3). The analysis of the above data showed that S_I<3.5mV, S_{V1} >3.5mV and R_{V1}/S_{V1} ratio < 2.6 were excellent differential indices predicting VAs originating from the distal portion of summit-CV (Supplementary Table 1).

Correlation of R(S) wave amplitude and R/S ratio in leads I and V1 with the horizontal distance from the effective target to the summit-CV

The linear distance between the effective targets and the summit-CV opening was positively correlated with R_I, R_I/S_I, and S_{V1}, but negatively correlated with S_I, R_V, and R_{V1}/S_{V1}. In other words, the more distal VAs origin in summit-CV, the larger the R_I amplitude, the smaller the S_I amplitude, and the larger the RI/SI ratio. Conversely, a smaller R_{V1} amplitude, a larger S_{V1} amplitude, and a smaller R_I/S_I ratio were observed. The analysis of the above data showed a more positive wave in lead I ($r=0.893$) and a more negative wave in lead V_1 ($r=0.764$) indicating a more distal origin in summit-CV (Fig. 4).

The typical cases of VAs originating from different portions of summit-CV are shown in Figs. 5 and 6.

Discussion

Major findings

This was the first study that comprehensively investigated ECG and electrophysiological features of idiopathic VAs originating from the different portions of summit-CV. Though the proximal summit-CV and distal summit-CV VAs showed similar ECG characteristics in the majority of leads, there was a significant difference between lead V_1 and lead I. S_I<3.5mV, S_{V1} >3.5mV and R_{V1}/S_{V1}<2.6 can be used to recognize VAs from the distal portion of summit-CV. A more positive wave in lead I and a negative wave in lead V_1 indicated more distal origin in summit-CV.

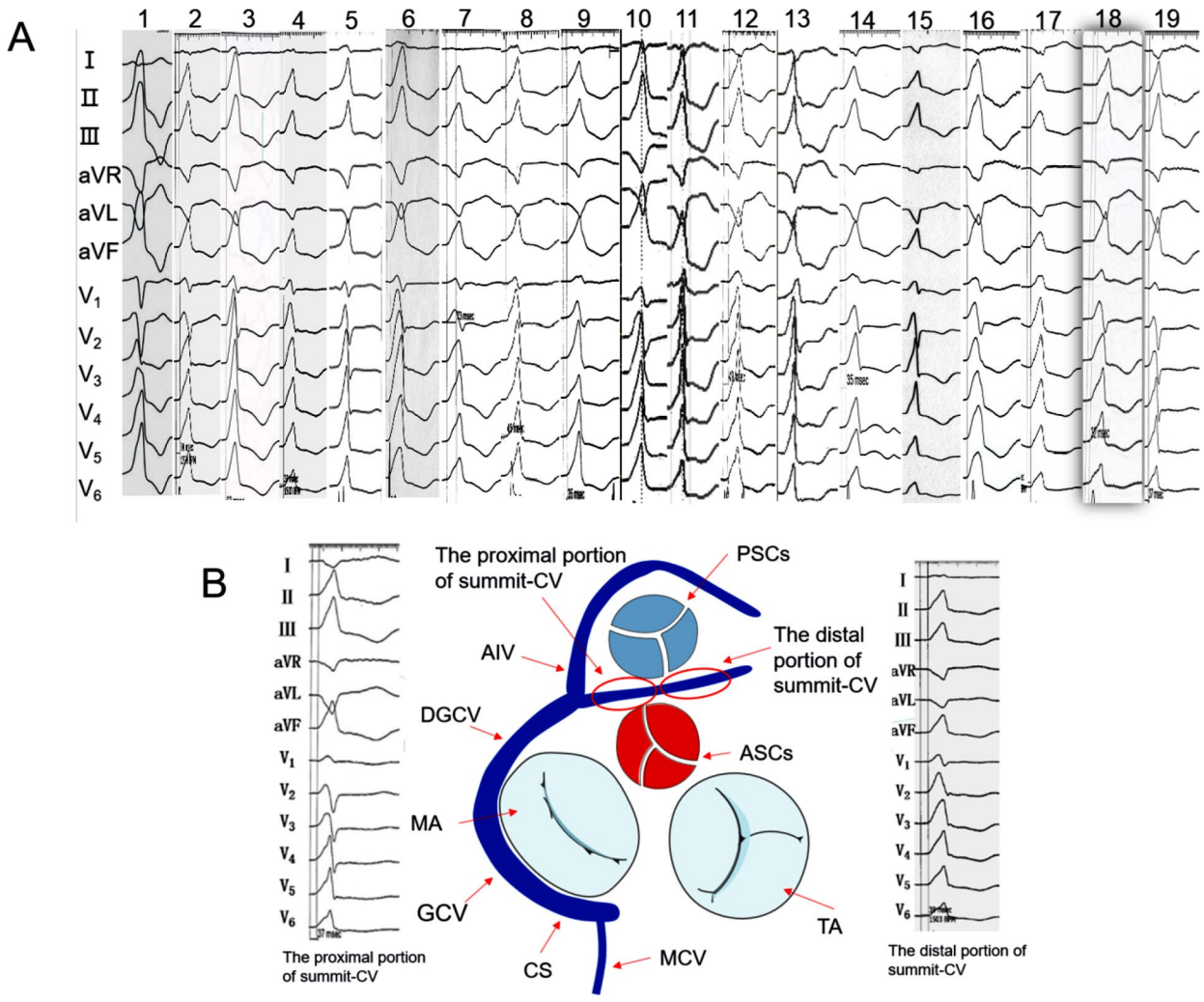

Fig. 2 **A**: ECG Characteristics of 19 patients with PVC originating from summit-CV (distal portion 1 to 8, proximal portion 9 to 19). **B**: Comparison of ECG characteristics of PVCs originating from the proximal and distal portions of the summit-CV. CS, coronary sinus; GCV, great cardiac vein; MCV, middle cardiac vein; DGCV, distal great cardiac vein; AIV, anterior interventricular vein; Summit-CV, communicating vein of the left ventricular summit; MA, mitral valve; TA, tricuspid valve; ASC, aortic sinus cusp; PSC, pulmonary sinus cusp

The left ventricular summit (LVS) was the most superior portion of the epicardial LV outflow tract, frequently identified as a primary source of IVAs. Recent studies revealed that the communicating vein connecting the great cardiac vein and the small cardiac venous systems passed between the aortic and pulmonary annulus. This vein was closely situated near the left ventricular summit (summit-CV) and could be effectively mapped and ablated for VAs originating from the LVS.

ECG characteristics of VAs originating from the summit-CV

Although ECG characteristics involving summit-CV VA origin have been reported, there are no relevant reports on the differences in ECG characteristics of VA originating from different portions of summit-CV [2, 6, 7]. Komatsu et al. [8]. reported the electrocardiogram characteristics of VAs originating from summit-CV, which showed an inferior axis with a monomorphic R pattern in inferior leads, and exhibited a nonspecific bundle branch block. All summit-CV VAs displayed a QS pattern in leads aVR and aVL, and had an R wave in lead V_1 with an R/S ratio of 0.67 ± 0.33 and no S wave in leads V_5 and V_6. The patients in our study showed similar ECG characteristics. However, regarding the R/S ratio in lead V1, we observed some different findings. An R/S ratio ≥ 2.6 in lead V_1 indicated proximal summit-CV VAs, while a ratio<2.6 indicated distal summit-CV VAs. We found more distal summit-CV VAs in their study, where a 2 F microcatheter was introduced into the summit-CV, which could assist in identifying more distal summit-CV VAs. Different from them, summit-CV VAs in our study were confirmed by a 4-mm irrigated catheter tip. Because of the larger size of the catheter tip, which prevented deep engagement in the thin lumen of the summit

Table 3 Comparison of mapping and ablation results between the two groups (n, %)

	Activation mapping V-QRS time (ms)	Pacing similarity (%)	Ablation attempts	Discharge time (s)	Operation time (min)	X-ray exposure time (min)	The distance from summit-CV opening (mm)*	A/V ratio			Specific potential				pacing capture		
								>1	=1	<1	Presystolic short-duration fractionated potential	Presystolic long-duration multicomponent fractionated potential	Presystolic isolated discrete potential	Presystolic high-amplitude discrete potential	Ventricular capture	Atrial capture	Loss of capture
The proximal group ($n=11$)	-35.7±6.6	96.9±2.4	4.3±0.6	145.6±58.3	73.3±9.5	13.7±2.8	6.82±2.11	0	4 (36.36)	7 (63.64)	2 (18.18)	4 (36.36)	1 (9.09)	2 (18.18)	10 (90.91)	0	1 (9.09)
The distal group ($n=8$)	-36.3±5.8	96.6±2.3	4.5±0.7	158.6±62.5	78.6±10.2	14.6±3.3	13.61±2.34	0	0	8 (100.00)	2 (25.00)	3 (37.50)	1 (12.50)	1 (12.50)	7 (87.50)	0	1 (12.50)
χ^2 or t	0.3760	0.7713	0.3207	0.1216	2.3510	0.6145	6.1287	/			/	/	/	/	/	/	/
p	>0.5	0.45	>0.5	>0.5	0.03	>0.5	0.000	>0.05			>0.05				>0.05		

* Horizontal distance between target sites in summit-CV and the intersection of DGCV and AIV.

CV, it was reasonable to speculate that the VAs ablated in our study were relatively more proximal than theirs. Otherwise, our study demonstrated that a more positive and less negative wave in lead I indicated a more distal origin in summit-CV. The mechanism of the above ECG characteristics of VA was considered. We supposed that distal summit-CV VAs owned a more rightward vector than proximal summit-CV VAs and depolarized in a similar direction to lead I, which induced a relatively more positive and less negative wave in the lead I. Moreover, for lead V_1, as the distal summit-CV located more adjacent to lead V1, its depolarization deviated from lead V_1, inscribed less positive wave and more negative wave, as proximal summit-CV more distal to lead V_1, it depolarized partially towards lead V_1, inscribed a more positive wave and less negative wave.

Mapping and ablation

Successful ablation of summit-CV VA was affected by many factors, such as the small size of the vessel lumen, high impedance within the CVS, tortuous course of the coronary venous system, and adjacence to the coronary artery [9–11]. Komatsu et al. [8]. described using a 2 F multipolar microcatheter introduced into the summit communicating veins to assist mapping and ablation in summit-CV. The 2 F microcatheter detected local ventricular activation earlier than the ablation catheter on the endocardial surface, confirming that the premature ventricular beat originates from the summit-CV. However, notably, in none of the summit-CV cases, it was possible to target the arrhythmia with direct ablation at the site of earliest activation. This limitation was primarily due to the vein being too small to accommodate a mapping/ablation catheter. Therefore, an anatomic approach applying radiofrequency energy at anatomically adjacent sites was used instead. However, the inability to directly ablate the earliest site within the summit-CV leads to a lower success rate of ablation procedures and a higher rate of recurrence. As such, in clinical practice, we still suggest targeting the earliest site reachable in summit-CV with a standard ablation catheter. Several novel ablation modalities could be considered to eliminate the Summit-CV VAs. Bipolar radiofrequency ablation, with a diagnostic catheter positioned in the narrow lumen of the Summit CV and an irrigated ablation catheter placed in the endocardium, may be available to treat Summit CV VAs [12]. Lesions produced with bipolar energy usually had a concentrated structure due to the vector of the radiofrequency current being redirected into the deep myocardium [13]. However, it had to be noted that there was a high risk of cardiac steam pop and cardiac rupture, as the diagnostic catheter did not have a temperature monitoring function. Ethanol ablation was also reported as a method for treating LVS VAs [14, 15]. Nonetheless,

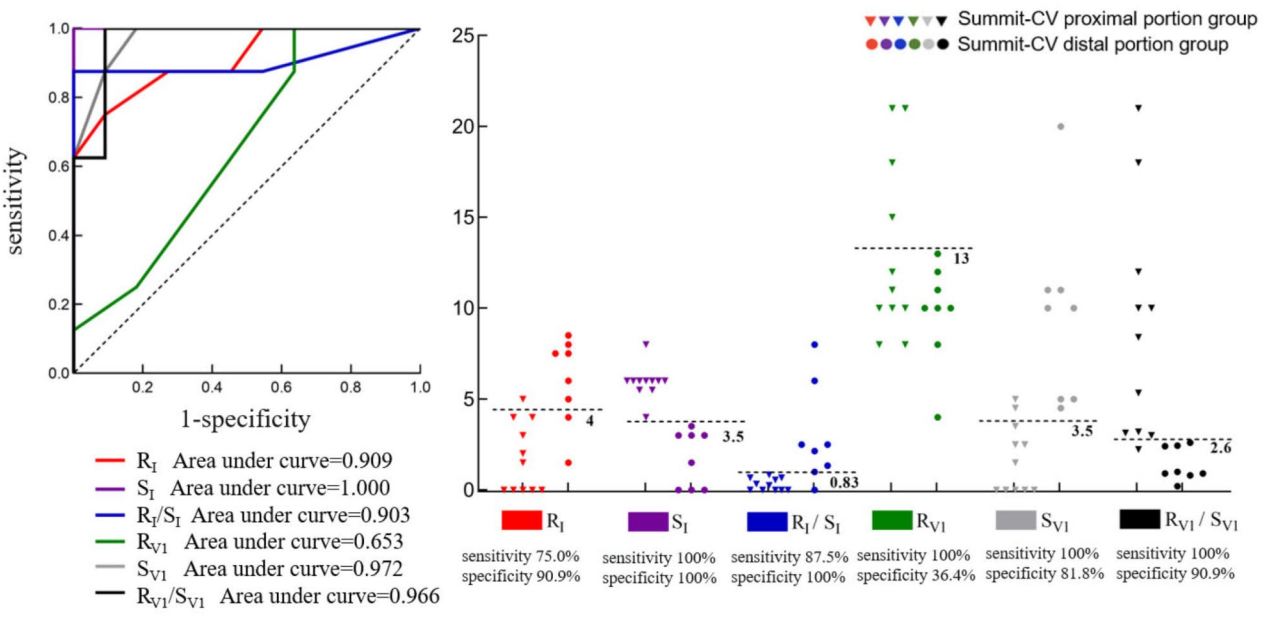

Fig. 3 ROC curves and scatter plots of R(S) wave amplitude and R/S ratio in leads I and V_1

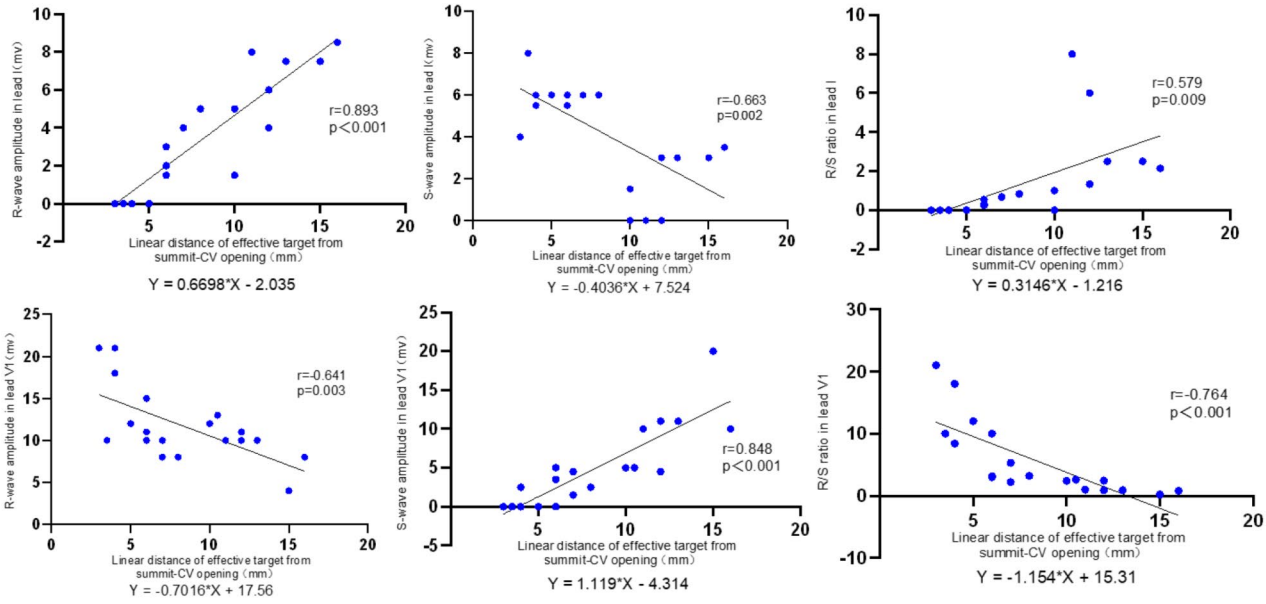

Fig. 4 Linear correlation analysis of R(S) wave amplitude and R/S ratio in leads I and V_1 with the linear distance between the effective target and summit-CV opening. The linear distance between the VAs origin and summit-CV opening (mm) was taken as the X-axis, and R (S) wave amplitude (mV) and R/S ratio (both expressed as absolute value) in leads I and V_1 were taken as the Y-axis for linear correlation analysis

potential catastrophic complications, such as coronary artery damage and atrioventricular block, had to be closely monitored.

In our study, the electrophysiological characteristics of different portions of summit-CV were investigated, including the A/V ratio, pacing-induced ventricle capture rate, and initial special bi-EGM potential. No significant difference was detected regarding these items. Anatomically, the left atrial appendage overlaid the LVS and was near the summit-CV. The A wave recorded in the target site of summit-CV during sinus rhythm was the far-field potential of the nearby left atrial appendage. Therefore, the A wave amplitude and A/V ratio in the target site were mainly dependent on the anatomical relationship between summit-CV and left atrial appendage rather than the location of the target site in summit-CV. The target sites in different portions of summit-CV showed similar pacing-induced ventricle capture

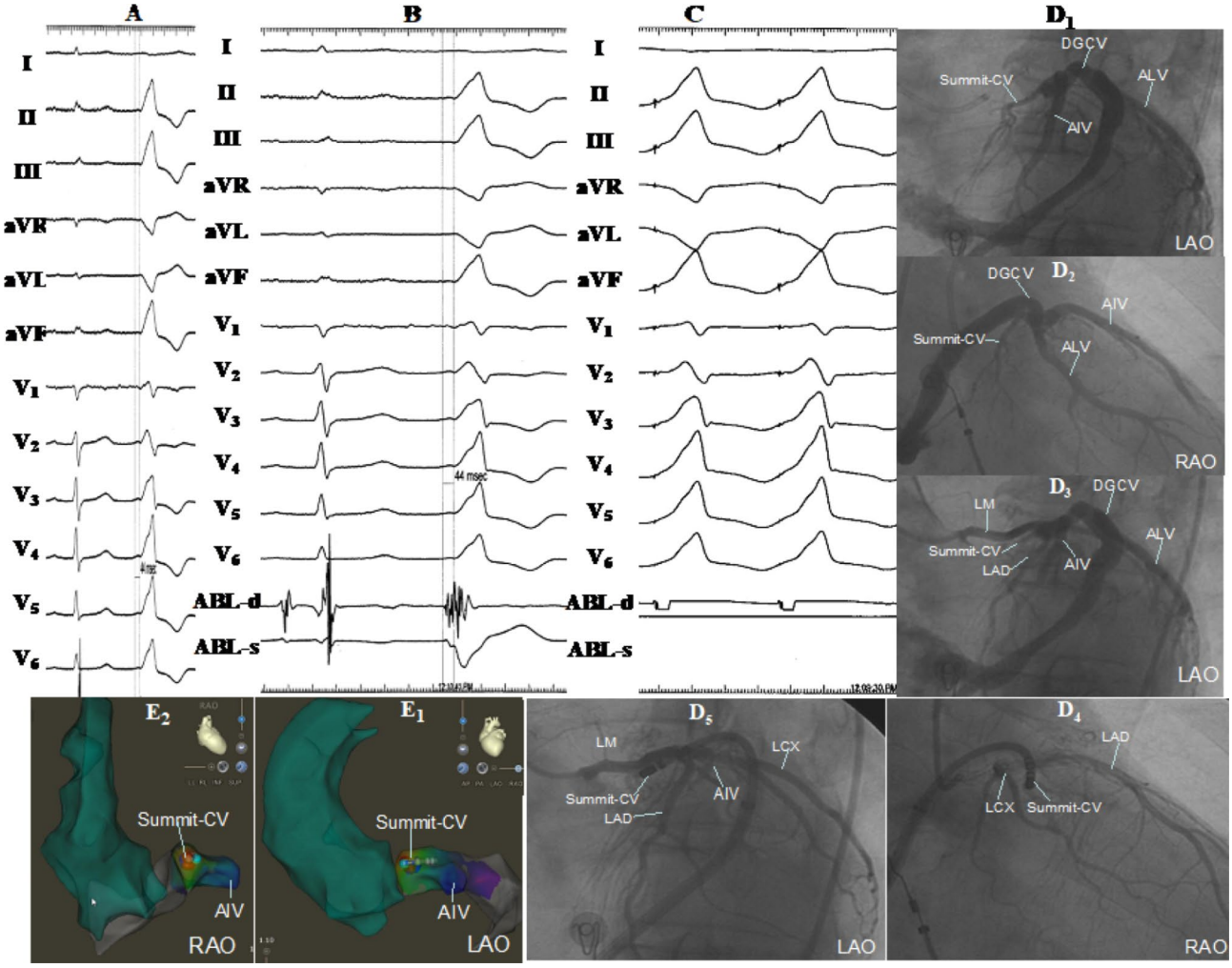

Fig. 5 ECG, the bipolar intracardiac electrograms and three-dimensional and X-ray imaging characteristics of PVC in the distal portion of the summit-CV. The surface ECG characteristics of PVC showed no ideal target site during mapping, such as the left and right ventricular outflow tracts (**A**). A multi-peak, high-amplitude, and long-duration clustered fragmented V wave (preceded surface ECG by 44 milliseconds) was detected at the distal portion of summit-CV, which showed small A and large V wave during bipolar mapping of sinus rhythm and PVC (**B**). Pacing mapping showed that the pacing-induced QRS was precisely the same as spontaneous PVC (**C**). X-ray images and three-dimensional mapping showed that the catheter was in the distal portion of summit-CV (**D**, **E**). The energy of 43 °C, 30 W was delivered on this site for about 8 s (the released energy was only 8 ~ 12 W), PVC disappeared, and additional ablation of 90 s was performed. However, the PVC recovered after 15 min of observation, so the temperature control was increased to 46 °C, and the energy release could reach 15 ~ 20 W, and the PVC disappeared, additional energy delivery for 100 s was performed. The patient was followed up for 6 years without recurrence. LAD, left anterior descending artery; LCX, left Circumflex artery; LM, left main artery; DGCV, distal great cardiac vein; AIV, anterior interventricular vein; Summit-CV, communicating vein of the left ventricular summit; ALV, anterolateral vein; ABL, ablation catheter; LAO, left anterior oblique; RAO, right anterior oblique. The results of coronary venography alone (D1, D2), the results of coronary arterio-venous double angiography (D3), and the results of selective coronary arterio-venous double angiography with ablation catheter (D4, D5)

rates. The summit-CV originated from the intersection between DGCV and AIV, drained into the small cardiac vein, and ran between the atrium and ventricle. When the target site in summit-CV was closer to the ventricle side than the atrium, pacing at the target site resulted in ventricular capture. Conversely, it lost ventricular capture when the target site was closer to the atrium side. As a result, pacing-induced ventricle capture of target sites was determined by vessel course to the atrium and ventricle, rather than whether it was in the distal or proximal portion. Finally, target sites in different portions of summit-CV present similar special bi-EGM characteristics. In our previous study, 41.07% of DGCV VAs showed bi-EGM of presystolic long-duration multicomponent fractionated potential [4]. It was speculated that the DGCV was the site where the ventricular myocardium interlaced with the atrium myocardium, holding a complex anatomy with various types of merged tissues. VAs originating from DGCV had to traverse various tissues, such as the vascular smooth muscle and myocardium, and overcome large impedance when conducting from epicardium to endocardium which led to the inequality

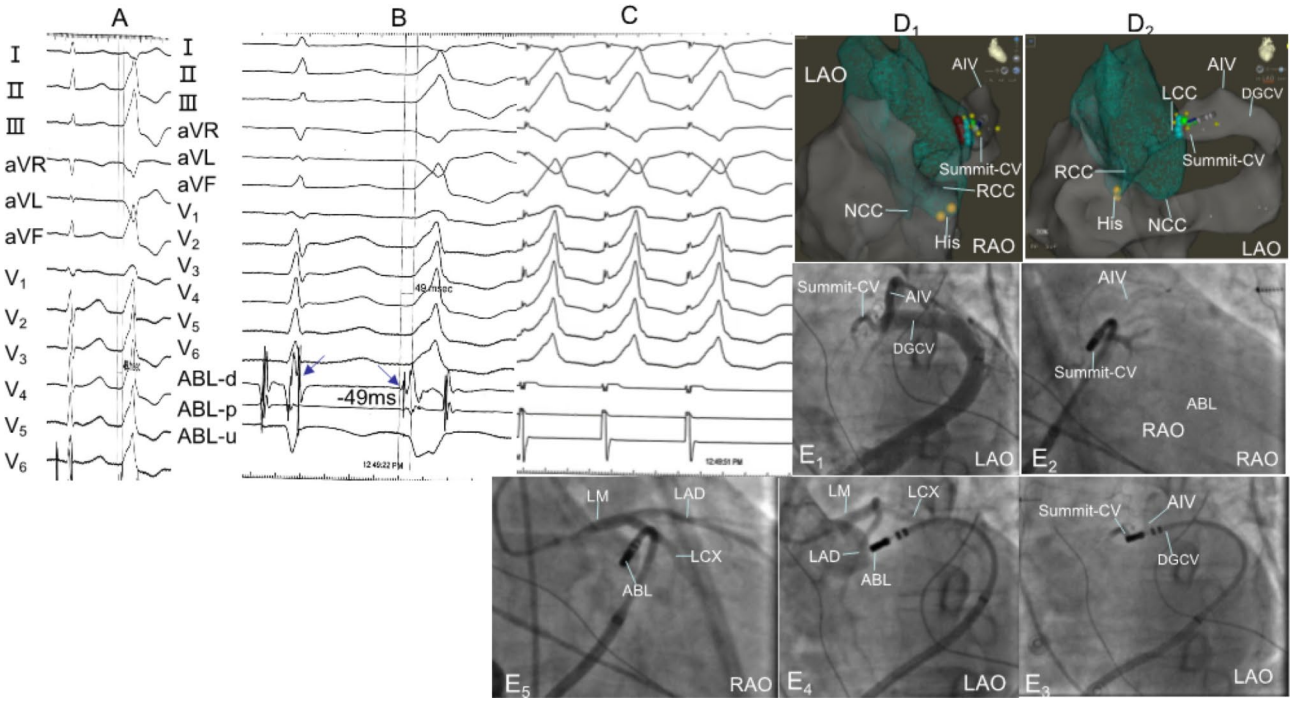

Fig. 6 ECG, the bipolar intracardiac electrograms, and three-dimensional and X-ray imaging characteristics of PVC in the proximal portion of summit-CV. PVC surface ECG characteristics (**A**). The QRS complex was mapped in the proximal portion of summit-CV, 49 milliseconds earlier than the surface ECG (**B**). During PVC, the target site showed a single-peaked, high-amplitude, and short-duration potential at the onset of the QRS complex, where a large A and large V (A/V = 1) were presented during sinus rhythm. Pacing-induced QRS complex was 99.1% identical to spontaneous PVC (**C**). X-ray images and three-dimensional mapping showed that the catheter was in the proximal portion of summit-CV (**D**, **E**). We presented the temperature control to 43 °C, energy 30 W, and impedance 300Ω to attempt ablation for about 6 s, then PVC disappeared (green dots were effective targets). Consolidation ablation 90 s and no recurrence of PVC was observed 30 min after the operation. The patient was followed up for 1 year without recurrence. LAD, left anterior descending artery; LCX, left Circumflex artery; LM, left main artery; DGCV, distal great cardiac vein; AIV, anterior interventricular vein; Summit-CV, communicating vein of the left ventricular summit; ABL, ablation catheter; LAO, left anterior oblique; RAO, right anterior oblique. The results of coronary venography alone (E1), the results of selective coronary venography with ablation catheters (E2, E3), and the results of coronary angiography (E4, E5)

of electricity and more possibility of presystolic long-duration multicomponent fractionated potential [9, 16, 17]. The summit-CV was an extended branch of DGCV; thus, summit-CV VAs exhibited similar bi-EGM characteristics to DGCV VAs, with presystolic long-duration multicomponent fractionated potential more observed.

Study limitations

First, this was a single-center, retrospective, and non-randomized clinical observational study. The sample size was small, and there may be sampling errors. We expect that sizeable multi-center cohort studies will be conducted in the future to validate our findings. Second, the distance between target sites in summit-CV and the intersection of DGCV and AIV was measured by X-ray measurement software, which may have some bias.

Conclusion

This study revealed the ECG characteristics of the VAs originating from the different portions of summit-CV. S_I<3.5mV, S_{V1} >3.5mV and R_{V1}/S_{V1}<2.6 can be used to recognize VAs from the distal portion of summit-CV. Correct identification of the distinctive features of these ECGs with regards to the anatomic location was important, which may help in successful ablation.

Supplementary Information

The online version contains supplementary material available at https://doi.org/10.1186/s12872-024-04099-0.

Supplementary Material 1

Acknowledgements

Not applicable

Author contributions

BS, CZ and JFL contributed to the conception and design of the study. BS, WMH and JMS organized the database and performed the statistical analysis. BS and WMH wrote the first draft of the manuscript. All authors contributed to the article and approved the submitted version. All authors reviewed the manuscript.

Funding

This work was supported by the National Natural Science Foundation of China [grant numbers 82070333]; the Zhejiang Provincial Natural Science Foundation [grant numbers LY21H020011]; the Wenzhou Municipal Science and Technology Commission [grant numbers ZY2020018, Y2020698]; the

Wenzhou Municipal Science and Technology Bureau [grant numbers, Y20220472].

Data availability
Statement in manuscript-Data are available on reasonable request to the corresponding author.

Declarations

Ethics statement
The patients/participants provided written informed consent to participate in this study. Written informed consent was obtained from the individual(s). The Ethics Committee of the Second Affiliated Hospital of Wenzhou Medical College approved the study (No.2022-02).

Disclosures
None.

Consent for publication
Not applicable.

Competing interests
The authors declare no competing interests.

Author details
[1]Department of Cardiology, Second Affiliated Hospital and Yuying Children's Hospital of Wenzhou Medical University, 325000 Wenzhou, China
[2]The First People's Hospital of Linping District, 311100 Hangzhou, China

Received: 12 February 2024 / Accepted: 6 August 2024
Published online: 13 August 2024

References

1. Mountantonakis SE, Frankel DS, Tschabrunn CM, Hutchinson MD, Riley MP, Lin D, et al. Ventricular arrhythmias from the coronary venous system: prevalence, mapping, and ablation. Heart Rhythm. 2015;12(6):1145–53.
2. Lin YN, Xu J, Pan YQ, Zheng C, Lin JX, Li J, et al. An electrocardiographic sign of idiopathic ventricular tachycardia ablatable from the distal great cardiac vein. Heart Rhythm. 2020;17(6):905–14.
3. Chen YR, Lin YF, Xu Q, Zheng C, He RL, Li J et al. Overcoming high impedance in the Transitional Area of the Distal Great Cardiac Vein during Radiofrequency catheter ablation of ventricular arrhythmia. J Cardiovasc Dev Dis 2022; 9(8).
4. Li J, Lin W, Zheng C, Zhang C, Yu J, Lin J. Implication of the distinctive bipolar intracardiac electrograms for ventricular arrhythmias arising from different regions of ventricular outflow tract. Europace. 2020;22(9):1367–75.
5. Hachiya H, Hirao K, Sasaki T, Higuchi K, Hayashi T, Tanaka Y, et al. Novel ECG predictor of difficult cases of outflow tract ventricular tachycardia: peak deflection index on an inferior lead. Circ J. 2010;74(2):256–61.
6. Baman TS, Ilg KJ, Gupta SK, Good E, Chugh A, Jongnarangsin K, et al. Mapping and ablation of epicardial idiopathic ventricular arrhythmias from within the coronary venous system. Circ Arrhythm Electrophysiol. 2010;3(3):274–9.
7. Hachiya H, Hirao K, Nakamura H, Taniguchi H, Miyazaki S, Komatsu Y, et al. Electrocardiographic characteristics differentiating epicardial outflow tract-ventricular arrhythmias originating from the anterior interventricular vein and distal great cardiac vein. Circ J. 2015;79(11):2335–44.
8. Komatsu Y, Nogami A, Shinoda Y, Masuda K, Machino T, Kuroki K, et al. Idiopathic ventricular Arrhythmias originating from the vicinity of the communicating vein of cardiac venous systems at the Left Ventricular Summit. Circ Arrhythm Electrophysiol. 2018;11(1):e005386.
9. Li YC, Lin JF, Li J, Ji KT, Lin JX. Catheter ablation of idiopathic ventricular arrhythmias originating from left ventricular epicardium adjacent to the transitional area from the great cardiac vein to the anterior interventricular vein. Int J Cardiol. 2013;167(6):2673–81.
10. Chen YH, Lin JF. Catheter ablation of idiopathic epicardial ventricular Arrhythmias originating from the vicinity of the coronary sinus system. J Cardiovasc Electrophysiol. 2015;26(10):1160–7.
11. d'Avila A, Houghtaling C, Gutierrez P, Vragovic O, Ruskin JN, Josephson ME, et al. Catheter ablation of ventricular epicardial tissue: a comparison of standard and cooled-tip radiofrequency energy. Circulation. 2004;109(19):2363–9.
12. Futyma P, Sauer WH. Bipolar Radiofrequency catheter ablation of Left Ventricular Summit arrhythmias. Card Electrophysiol Clin. 2023;15(1):57–62.
13. Futyma P, Sander J, Ciapala K, Gluszczyk R, Wysokinska A, Futyma M, et al. Bipolar radiofrequency ablation delivered from coronary veins and adjacent endocardium for treatment of refractory left ventricular summit arrhythmias. J Interv Card Electrophysiol. 2020;58(3):307–13.
14. Tavares L, Fuentes S, Lador A, Da-Wariboko A, Wang S, Schurmann PA, et al. Venous anatomy of the left ventricular summit: therapeutic implications for ethanol infusion. Heart Rhythm. 2021;18(9):1557–65.
15. Tokuda M, Sobieszczyk P, Eisenhauer AC, Kojodjojo P, Inada K, Koplan BA, et al. Transcoronary ethanol ablation for recurrent ventricular tachycardia after failed catheter ablation: an update. Circ Arrhythm Electrophysiol. 2011;4(6):889–96.
16. Spencer JH, Anderson SE, Iaizzo PA. Human coronary venous anatomy: implications for interventions. J Cardiovasc Transl Res. 2013;6(2):208–17.
17. Sorgente A, Epicoco G, Ali H, Foresti S, De Ambroggi G, Balla C, et al. Negative concordance pattern in bipolar and unipolar recordings: an additional mapping criterion to localize the site of origin of focal ventricular arrhythmias. Heart Rhythm. 2016;13(2):519–26.

Publisher's Note